



Decoupling between bacterial production and primary production over multiple time scales in the North Pacific Subtropical Gyre

Donn A. Viviani^{a,b,*}, Matthew J. Church^{a,b,1}

^a Department of Oceanography, University of Hawaii at Manoa, Honolulu, HI, USA

^b Center for Microbial Oceanography: Research and Education, University of Hawaii, Honolulu, HI, USA

ARTICLE INFO

Keywords:

³H-leucine incorporation
Primary production
Time-series
North Pacific Ocean
Station ALOHA

ABSTRACT

We measured rates of ³H-leucine (³H-Leu) incorporation, as a proxy for bacterial production, at Station ALOHA (22°45'N, 158°W) in the oligotrophic North Pacific Subtropical Gyre (NPSG). We report measurements conducted between January 2011 and April 2013, examining variability in ³H-Leu incorporation over diel, daily, and monthly time scales. Rates of ³H-Leu were evaluated in the context of contemporaneous ¹⁴C-based primary productivity (¹⁴C-PP) to identify potential temporal coupling between these measures of productivity. Throughout the upper ocean (0–125 m), rates of ³H-Leu incorporation measured in the light (³H-Leu_{Light}) were stimulated (1.5-fold, on average) relative to measurements in the dark (³H-Leu_{Dark}). At monthly scales, rates of ³H-Leu_{Light} and ³H-Leu_{Dark} varied 4.9-fold and 3.8-fold, respectively, while rates of ¹⁴C-PP varied 1.7-fold. Rates of ¹⁴C-PP were often elevated during summer months (May through August) when incident light flux was greatest, while rates of both ³H-Leu_{Light} and ³H-Leu_{Dark} often peaked in early fall (August through October) when seawater temperatures were maximal. Near-daily measurements of ³H-Leu incorporation and ¹⁴C-PP conducted over a 62-day period in the summer of 2012 revealed that rates of ³H-Leu_{Light} and ³H-Leu_{Dark} varied ~2.5 and 2.0-fold, respectively, similar to ~1.8-fold daily variability observed in rates of ¹⁴C-PP. Over diel time scales, rates of ³H-Leu_{Light} and ³H-Leu_{Dark} demonstrated different patterns, with rates of ³H-Leu_{Light} elevated at mid-day and rates of ³H-Leu_{Dark} greatest in the early evening. Together, these results suggest that in this oligotrophic ecosystem, photosynthetic production of organic matter and bacterial production can be temporally uncoupled across daily to seasonal scales.

1. Introduction

The ocean supports nearly half of global net primary productivity (PP), with much of that production occurring in the oligotrophic gyres of the open ocean (Behrenfeld and Falkowski, 1997; Field et al., 1998). A significant fraction of this photosynthetically-fixed carbon supports the growth and metabolic activities of bacterioplankton (del Giorgio et al., 1997; Duarte and Cebrian, 1996; Ducklow and Carlson, 1992). Bacterial production (BP) of biomass is a central component of aquatic food webs (Azam et al., 1983; Pomeroy, 1974), estimated to account for 10–15% of net PP in open ocean ecosystems (Ducklow, 1999; Ducklow and Carlson, 1992), with bacterial demand for organic matter (inclusive of requirements for biomass production and respiration) accounting for > 70% of contemporaneous rates of primary production (Church, 2008; Kirchman, 2004). Hence, estimates of the magnitude and variability associated with bacterial growth in the sea are critical to understanding ocean carbon cycling.

Examining spatiotemporal coupling between BP and PP provides insight into the relative dependence of bacterial growth on contemporaneous phytoplankton production. The nature of the coupling between BP and PP is generally quantified based on correlative or regression analyses (Ducklow and Carlson, 1992; Joint and Pomroy, 1987). Such analyses provide insight into the strength of coupling between photosynthetic production of organic matter and its consumption by heterotrophic bacteria (Billen et al., 1990; Ducklow and Carlson, 1992). The nature of such coupling can be regulated by numerous processes, including availability of inorganic and organic nutrients, grazing pressure, and temperature (Alonso-Sáez et al., 2008; Billen et al., 1990; Carlson et al., 1996; Cotner and Biddanda, 2002; Fouilland et al., 2014; Shiah and Ducklow, 1994). To date there are few studies examining temporal coupling between BP and PP in open ocean ecosystems (although see Carlson et al., 1996; Ducklow and Carlson, 1992; Ducklow et al., 2012; Steinberg et al., 2001; Van Wambeke et al., 2008); this coupling has also been examined in coastal, estuarine, and

* Correspondence to: University of Hawaii at Manoa, Department of Oceanography, 1950 East-West Road, Honolulu, HI 96822, USA.

E-mail address: viviani@hawaii.edu (D.A. Viviani).

¹ Current address: Flathead Lake Biological Station, University of Montana, Polson, MT, USA.

freshwater systems (e.g. Fuhrman et al., 1985; Pace and Cole, 1994; Shiah and Ducklow, 1994). Some of these studies describe significant positive correlations between BP and PP; however, the nature of these relationships can be complicated by lagged responses in BP relative to PP (e.g. Steinberg et al., 2001). For example, at the Bermuda Atlantic Time-series Study (BATS) in the Sargasso Sea, rates of BP demonstrate weak to moderate seasonality, generally increasing 2–3-fold during mid-summer and declining into fall and winter (Carlson et al., 1996; Steinberg et al., 2001). In contrast, rates of ^{14}C -primary production (^{14}C -PP) demonstrate relatively strong seasonality, varying up to 5-fold over the year, peaking in early spring (Michaels et al., 1994; Steinberg et al., 2001). The seasonal-scale decoupling of PP and BP in this ecosystem coincides with patterns in the production and removal of dissolved organic carbon (DOC), resulting in concentrations of DOC increasing throughout the spring and summer (Carlson et al., 1994; Hansell and Carlson, 1998). Such seasonal-scale decoupling in ^{14}C -PP and BP in this ecosystem results in net production of DOC, which is available for subsequent export (via convective mixing) during the winter (Carlson et al., 1994). Hence, the coupling between contemporaneous ^{14}C -PP and BP plays potentially important roles in carbon export and cycling.

Since 1988, the Hawaii Ocean Time-series (HOT) program has conducted near-monthly measurements of ocean biogeochemistry and hydrography at the open ocean field site Station ALOHA (22°45'N, 158°00'W) in the North Pacific Subtropical Gyre (NPSG). This ecosystem is characterized by a deep euphotic zone (the depth to which 1% of the surface light flux penetrates at Station ALOHA averages 105 ± 10 m), persistently low concentrations of inorganic nutrients, and picoplankton ($< 2 \mu\text{m}$) comprising a large fraction of upper ocean biomass (Campbell et al., 1994; Rii et al., 2016). Moreover, rates of PP in this ecosystem appear sustained in large part by intensive recycling of nutrients through the metabolic activities of planktonic microorganisms (Karl, 1999). HOT program measurements of ^{14}C -PP reveal significant seasonality, with rates increasing 2–3-fold in summer, coincident with increased insolation (Church et al., 2013; Karl et al., 2012; Letelier et al., 2004). Despite these seasonal-scale increases in ^{14}C -PP, rates of photosynthetic production of DOC (as measured by production of extracellular ^{14}C -DOC) do not demonstrate significant seasonality or apparent relationships to rates of ^{14}C -PP (Viviani et al., 2015). To date however, less is known about temporal variability in BP, or possible relationships between rates of BP and PP in this ecosystem. Previous work at ALOHA has demonstrated that sunlight stimulates rates of ^3H -leucine (^3H -Leu) incorporation (Church et al., 2006, 2004), a proxy for BP, an effect that appears largely driven by incorporation of ^3H -Leu by the unicellular cyanobacterium *Prochlorococcus* (Björkman et al., 2015; Church et al., 2006, 2004).

In this study, we measured rates of ^3H -Leu incorporation and ^{14}C -PP over diel to near-monthly time scales at Station ALOHA. Doing so allowed us to evaluate potential coupling between BP and PP over a range of time scales and provided insight into factors controlling these processes in this persistently oligotrophic habitat.

2. Methods

2.1. ^{14}C -primary production and ^3H -leucine incorporation measurements

Samples were collected at or in the vicinity of Station ALOHA on 24 different cruises between January 2011 and April 2013. On each cruise, rates of ^3H -Leu incorporation into protein were measured (Kirchman et al., 1985; Simon and Azam, 1989). Coincident measurements of plankton assimilation of ^{14}C -bicarbonate were utilized as a proxy for net PP (Marra, 2009; Steemann Nielsen, 1952). Seawater samples for both measurements of production were collected from pre-dawn vertical hydrocasts at 6 discrete depths (5, 25, 45, 75, 100, 125 m) using polyvinyl chloride sampling bottles affixed to a rosette sampler

equipped with Sea-Bird 911+ conductivity, temperature, and depth (CTD) sensors (Karl and Lukas, 1996). Measurements of ^{14}C -PP were conducted following HOT program protocols (Letelier et al., 1996). Briefly, seawater was subsampled under subdued light from the rosette sampling bottles into triplicate acid-cleaned 500 ml polycarbonate bottles. Samples were inoculated with ^{14}C -bicarbonate to a final activity of ~ 1.85 MBq, affixed to a free-drifting array, and incubated *in situ* over the full photoperiod (ranging 11–13 h). During the summer of 2012, rates of ^{14}C -PP were measured daily as part of the Center for Microbial Oceanography: Research and Education (C-MORE) HOE-DYLAN cruises. For these near-daily scale measurements, seawater was collected at 25 m from a predawn CTD rosette cast; triplicate 500 ml polycarbonate bottles were filled from the CTD rosette bottles, inoculated with ~ 1.85 MBq ^{14}C -bicarbonate, and placed for the duration of the photoperiod in a seawater-cooled, deckboard incubator, shaded with blue Plexiglass to $\sim 30\%$ of surface irradiance.

At the end of the photoperiod, bottles were retrieved from the incubator or the *in situ* array, and 250 μl was subsampled from each sample bottle into a 20 ml glass scintillation vial containing 500 μl of β -phenethylamine for subsequent determination of the total activity of ^{14}C added to each sample. The remaining sample volume was gently vacuum filtered onto 25 mm diameter glass fiber filters (Whatman GF/F). Filters were placed in glass 20 ml scintillation vials and stored frozen until analysis. At the shore-based laboratory, filters were thawed and 1 ml of 2 mol L^{-1} hydrochloric acid was added to each filter; filters were allowed to passively vent in a fume hood overnight. After venting, 10 ml of Ultima Gold (Perkin Elmer) liquid scintillation cocktail was added to each filter and to the total activity vials; vials were placed in a liquid scintillation counter for determination of the resulting ^{14}C activities. Samples were stored in the dark and recounted after a month; the values from the second counts were used to calculate rates of ^{14}C -PP (Karl et al., 1998).

Seawater for measurements of ^3H -Leu incorporation was collected from the same CTD hydrocasts and depths as coincident ^{14}C -PP measurements. Polyethylene amber bottles (125 ml capacity) were subsampled from the CTD rosette bottles, and duplicate acid-cleaned 12 ml polycarbonate centrifuge tubes (Nalgene Oak Ridge) were filled from each depth. Each polycarbonate tube was inoculated with 20 nmol L^{-1} (final concentration) 3,4,5- ^3H -leucine (Perkin Elmer; stock specific activities ranged from 108 to 144 Ci/mmol). An additional 1.5 ml per depth was subsampled into 2 ml microcentrifuge tubes (Axygen; Pace et al., 2004) containing 100 μl of 100% (w/v) ice-cold trichloroacetic acid (TCA) to serve as a killed blank. The polycarbonate sample tubes were capped and incubated *in situ* over the photoperiod to measure rates of ^3H -Leu incorporation in both dark (through use of black cloth bags; hereafter ^3H -Leu_{Dark}) and light (hereafter ^3H -Leu_{Light}) on the same free-drifting array utilized for the ^{14}C -PP measurements. At the end of the photoperiod, triplicate 1.5 ml subsamples were removed from each tube and added to 2 ml microcentrifuge tubes (Axygen) containing 100 μl of 100% ice-cold TCA; these tubes were stored frozen until analysis. Samples were processed following a modified method of the microcentrifuge method (Smith and Azam, 1992). Microcentrifuge tubes were spun at $\sim 23,900g$ for 15 min at 4 °C in a refrigerated microcentrifuge; supernatants were decanted, 1 ml ice-cold 5% TCA was added to each microcentrifuge tube and samples were spun for an additional 5 min at $\sim 23,900g$ at 4 °C. Supernatants were decanted and 1 ml of 80% ethanol was added to each sample, and tubes were spun for an additional 5 min at $\sim 23,900g$ at 4 °C. After decanting supernatants, samples were left uncapped for 12–16 h in a fume hood to evaporate any residual ethanol from the microcentrifuge tubes. When samples had completely dried, 1 ml of Ultima Gold LLT scintillation cocktail was added to each tube, the tubes were vortexed, placed into 7 ml polyethylene scintillation vials (serving as a carrier vials) and counted on a liquid scintillation counter.

During the summer of 2012, rates of ^3H -Leu incorporation were measured at near-daily time scales during a series of cruises to Station

ALOHA as part of the C-MORE HOE-DYLAN cruises. For these measurements, seawater samples from 25 m were collected from a pre-dawn CTD rosette cast; the seawater was transferred into 125 ml amber polyethylene bottles and triplicate 1.5 ml subsamples were added to 2 ml microcentrifuge tubes (Axygen) containing ^3H -Leu (20 nmol L^{-1} final concentration). Triplicate samples were incubated in the dark (inside a black cloth bag) and in the light using the same deckboard incubator used for ^{14}C -PP measurements. Blank (TCA killed) samples were prepared as previously described. In addition, we performed higher frequency “diel” sampling over a 48-h period (August 31 to September 1), in which 25 m samples were collected every four hours, and samples were incubated in the same deckboard incubator previously described. Measurements conducted during daylight hours included both dark and light incubations (as described previously), while nighttime incubations were only incubated in the dark. The resulting measured rates of ^3H -Leu incorporation were fit in MATLAB (Mathworks) using a nonlinear least squares fit to a sinusoidal model (John et al., 2011).

2.2. Time-course experiments to evaluate linearity of ^3H -leucine incorporation

Measurements of ^3H -Leu incorporation were conducted during the monthly HOT program cruises on the same free-drifting array used for measurements of ^{14}C -PP, allowing incubation of samples under *in situ* temperature and light conditions. However, this procedure resulted in relatively long incubation times (photoperiods ranging 11–13 h), and thus had the potential to underestimate ^3H -Leu incorporation rates due to increased likelihood of turnover of the ^3H -labeled protein pool (Kirchman et al., 1986). To evaluate potential non-linearity in rates of ^3H -Leu incorporation, we performed a series of time-course incubation experiments (April 2013, May 2013, June 2013, and May 2014). For these experiments, samples were incubated between 3 and 15 h to ascertain the period over which rates of ^3H -Leu incorporation into TCA insoluble macromolecules remained linear. Seawater (5 m and 25 m) was subsampled into amber polyethylene bottles from the CTD rosette; 1.5 ml subsamples were aliquoted into 2 ml microcentrifuge tubes (Axygen) and inoculated with 20 nmol L^{-1} (final concentration) ^3H -leucine. Samples were incubated in a surface seawater-cooled incubator, in both light and dark (as described previously), and triplicate 1.5 ml samples were sacrificed at regular intervals to evaluate the relationship between incubation time and ^3H activity (measured as disintegrations per minute, dpm).

Least squares regression analyses were used to evaluate the robustness of linear model fits to observations of ^3H -Leu incorporation over time; candidate models were chosen that included both linear and saturation phases. Akaike information criterion (AIC) scores (Burnham et al., 2010) were calculated and used to select the model with the best fit to the time-course activity measurements. We used the model with the best fit to determine the time period over which these incubation experiments remained linear. We then corrected for non-linearity deriving from incubation length for our measured rates of ^3H -Leu_{Dark} and ^3H -Leu_{Light} from *in situ* incubations on each cruise:

$$^3\text{H}\text{-Leu incorporation} = ^3\text{H}\text{-Leu}_{\text{measured}} + [\text{time of incubation} - \text{period of linearity}] \times (^3\text{H}\text{-Leu}_{\text{measured}} / \text{incubation period of linearity}) \quad (1)$$

where $^3\text{H}\text{-Leu}_{\text{measured}}$ is the rate of ^3H -Leu incorporation measured in the incubation, time of incubation is the duration of each incubation, and period of linearity (in hours) is the time over which the incorporation was linear.

2.3. Contextual measurements of light, cell abundances, and nutrients

The daily flux of incoming photosynthetically active radiation (PAR;

400–700 nm) was measured using a deckboard LI-COR LI-192 cosine collector. Vertical profiles of downwelling photosynthetically active radiation (PAR) were measured at noon using a Satlantic HyperPro radiometer; in addition, a deckboard radiometer (Satlantic) collected coincident measurements of incident PAR. These measurements were used to derive attenuation coefficients of PAR (K_{PAR}) for each cruise. Derived K_{PAR} values and incident surface irradiance were used to calculate daily light fluxes at specific depth horizons.

Cellular abundances of non-pigmented picoplankton and *Prochlorococcus* were enumerated by flow cytometry. Briefly, seawater samples were fixed with 0.25% final concentration of paraformaldehyde, flash frozen at -80°C , and analyzed using an Influx Mariner flow cytometer (Cytospeia) following standard HOT protocols (<http://hahana.soest.hawaii.edu/hot/methods/bact.html>). Inorganic nutrient concentrations (nitrate + nitrite, N+N and soluble reactive phosphorus, SRP) and chlorophyll *a* concentrations were collected and analyzed using standard HOT program protocols (Karl et al., 2001).

2.4. Statistical data analysis and carbon conversion

Seasonal binning of data was defined based on the solstice to equinox (*i.e.* Spring from March 20 to June 20; Summer from June 21 to September 22, Fall from September 23 to December 20, and Winter from December 21 to March 19). Depth-integrated (0–125 m) rates and stocks were calculated using trapezoidal integration. Statistical analyses and curve fitting were performed using MATLAB (Mathworks) or in the R statistical environment (R Development Core Team, 2008). Data that did not meet the assumptions of normality were \log_{10} transformed prior to analysis. For statistical treatment of ratios, geometric mean and standard deviations were used (Zar, 1999). Least squares linear regression analyses were utilized to examine potential temporal coupling between measured rates of ^{14}C -PP and ^3H -Leu. In addition, measurements of ^{14}C -PP, PAR, temperature, chlorophyll *a*, and picoplankton abundances were used for stepwise multiple linear regression analyses to examine how variability in habitat conditions influenced rates of BP. Stepwise multiple linear regressions were performed through sequential addition of terms to a linear model, retaining those terms whose inclusion resulted in a model with a *p*-value < 0.05; this procedure generated an *n*-order polynomial, where *n* is the number of terms successfully retained in the final model. We also examined our time-series for possible lags in the relationships between ^{14}C -PP and $^3\text{H}\text{-Leu}_{\text{Dark}}$ or $^3\text{H}\text{-Leu}_{\text{Light}}$ at daily scales (during the summer of 2012) and at monthly scales. For monthly lags, we binned rates of ^{14}C -PP, $^3\text{H}\text{-Leu}_{\text{Dark}}$, and $^3\text{H}\text{-Leu}_{\text{Light}}$ by month and then interrogated these monthly time-series for lagged relationships. Daily rates of ^3H -Leu incorporation were computed as the rate of $^3\text{H}\text{-Leu}_{\text{Light}}$ multiplied by the duration of the photoperiod, plus the rate of $^3\text{H}\text{-Leu}_{\text{Dark}}$ multiplied by the length of the nighttime period.

3. Results

The current study sought to examine temporal relationships between BP and PP at Station ALOHA in the persistently oligotrophic upper ocean (0–125 m) habitat of the NPSG. A total of 24 different cruises at or in the vicinity of Station ALOHA were sampled over an ~2-year period. Throughout the study, sea surface temperatures (SST) varied from 22.5 to 26.8°C , reaching an annual maximum in September and October, and minimum during the late winter (February and March). The mixed layer fluctuated between 34 and 126 m, with deeper mixed layers in the winter, followed by rapid shoaling and stratification through the spring to early fall (Fig. 1). Incident PAR fluctuated between 15.2 and $48.4 \text{ mol quanta m}^{-2} \text{ d}^{-1}$, with lower fluxes in the winter, increasing steadily from the spring into the summer (Fig. 1). Concentrations of inorganic nutrients (specifically N+N and SRP) were persistently low (averaging $4 \pm 2 \text{ nmol N L}^{-1}$ and $100 \pm 49 \text{ nmol P L}^{-1}$, respectively) in the well-lit regions (< 45 m) of

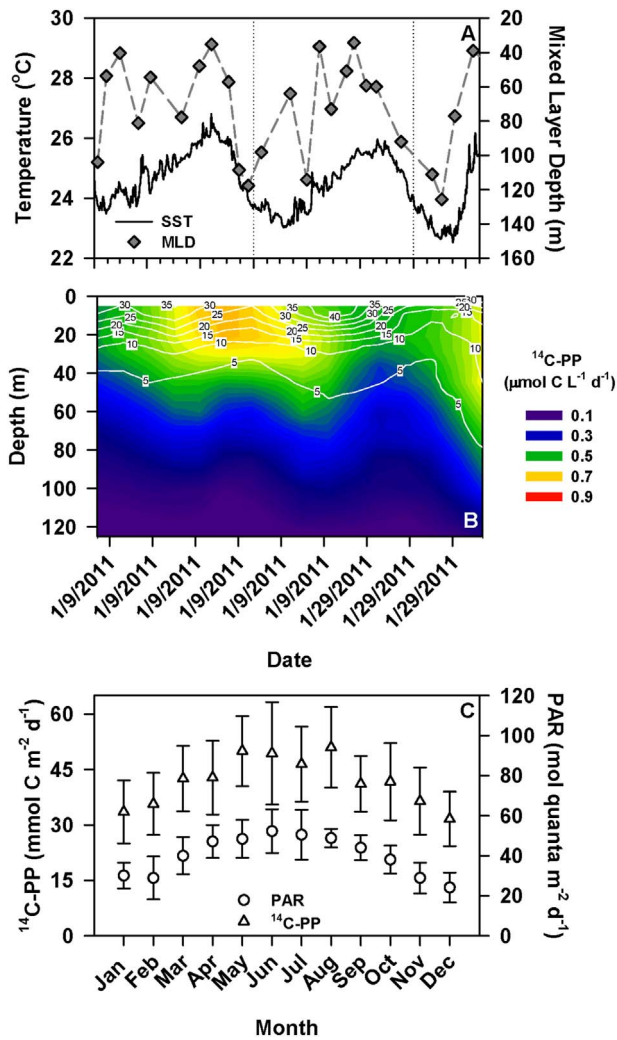


Fig. 1. Measurements of mixed layer depth (MLD) from HOT cruises and sea surface temperature (SST) from the WHOI Hawaii Ocean Time-series (WHOTS) mooring during this study (panel A). Rates of ¹⁴C-PP measured during this study (color contours; panel B) overlain by downwelling photosynthetically active radiation (PAR; in units of mol quanta m⁻² d⁻¹; white contours). The climatology of monthly-binned depth-integrated (0–125 m) rates of ¹⁴C-PP and surface PAR at Station ALOHA (panel C); error bars are one standard deviation of the time-averaged mean.

the upper ocean, with concentrations increasing sharply at depths below which PAR fluxes were < 5 mol quanta m⁻² d⁻¹. Rates of ¹⁴C-PP measured during this study (2011–2013) demonstrated depth-dependent patterns consistent with the historical HOT program measurements, with rates in the upper euphotic zone (0–45 m) approximately

3-fold greater than those in the lower euphotic zone (75–125 m; Fig. 1). When sampled at near-monthly time scales, depth-integrated (0–125 m) rates of ¹⁴C-PP varied less than 2-fold, ranging 2.7 and 4.6 mmol C m⁻² h⁻¹, with a major fraction (46–75%) of this production occurring in the upper 45 m of the water column (Table 1).

3.1. Time-course experiments to examine linearity in ³H-leucine incorporation

Use of *in situ* incubations for measuring rates of ³H-Leu incorporation and ¹⁴C-PP enabled mimicking of light and temperature conditions from depths where the samples were collected. To examine whether the incorporation of ³H-Leu remained linear over these photoperiod incubations (11–13 h), we conducted time-course experiments (incubations ranging from 3 to 16 h) in both the light and dark in deck-board incubators. Least-squares regression analyses were used to fit hyperbolic tangent models to the time-course measurements (Fig. 2). In these experiments ³H-Leu incorporation remained linear for 9 ± 2 h. Comparing the rates of ³H-Leu incorporation derived based on a linear fit over the initial ~9 h of these experiments to the hyperbolic tangent fit of the full photoperiod incubations (11–13 h), demonstrated that the photoperiod measurements underestimated both ³H-Leu_{Dark} and ³H-Leu_{Light} by 48–70%. The resulting regression analyses were used to correct rates of ³H-Leu_{Dark} and ³H-Leu_{Light} measured over the photoperiod.

3.2. Monthly-scale variability in rates of ³H-leucine incorporation

On near-monthly HOT cruises, rates of ³H-Leu incorporation were measured coincident with HOT program measurements of ¹⁴C-PP. Rates of both ³H-Leu_{Dark} and ³H-Leu_{Light} showed vertically-dependent patterns (Fig. 3), with depth-integrated rates significantly greater in the well-lit upper euphotic zone (0–45 m) compared to the lower euphotic zone (75–125 m; *t*-test; *p* < 0.0001; Table 1). Rates of both ³H-Leu_{Dark} and ³H-Leu_{Light} in the upper euphotic zone (< 45 m) ranged 3–15 pmol Leu L⁻¹ h⁻¹ and 4–26 pmol Leu L⁻¹ h⁻¹, respectively. In the lower euphotic zone (75–125 m) rates of ³H-Leu_{Dark} and ³H-Leu_{Light} ranged 1–10 pmol Leu L⁻¹ h⁻¹ and 1–15 pmol Leu L⁻¹ h⁻¹, respectively (Fig. 3). The ratio of ³H-Leu_{Light} to ³H-Leu_{Dark} (L:D ratio) averaged 1.5 throughout the euphotic zone (0–125 m) and demonstrated no significant depth-dependent pattern (one-way ANOVA, *p* > 0.05; Fig. 3). The difference between ³H-Leu_{Light} and ³H-Leu_{Dark} (ΔLeu; ΔLeu = ³H-Leu_{Light} - ³H-Leu_{Dark}) averaged 5 ± 3 pmol Leu L⁻¹ h⁻¹ in the upper euphotic zone, and 2 ± 3 pmol Leu L⁻¹ h⁻¹ in the lower euphotic zone. The resulting depth-integrated (0–125 m) rates of ³H-Leu_{Dark} ranged from 0.3 to 1.2 μmol Leu m⁻² h⁻¹ (averaging 0.7 ± 0.2 μmol Leu m⁻² h⁻¹), while the rates of ³H-Leu_{Light} varied between 0.4 and 1.9 μmol Leu m⁻² h⁻¹ (averaging 1.2 ± 0.4 μmol Leu m⁻² h⁻¹; Fig. 4). There were no significant interannual differences in the depth-integrated (0–125 m) rates of ³H-Leu_{Dark} measured in 2011 and 2012 (*t*-

Table 1

Depth-integrated stocks and rate measurements during this study, including mean ± standard deviation (SD) and ranges (in parenthesis) for rates of ³H-Leu_{Dark} and ³H-Leu_{Light} (nmol Leu m⁻² h⁻¹), abundances of *Prochlorococcus* (*Pro*) and non-pigmented picoplankton (non-pigs). Also shown are rates of ¹⁴C-PP (mmol C m⁻² h⁻¹) and the ratio of daily rates of BP to ¹⁴C-PP (as a percent).

Depth (m)	³ H-Leu _{Dark} (nmol Leu m ⁻² h ⁻¹)	³ H-Leu _{Light} (nmol Leu m ⁻² h ⁻¹)	<i>Pro</i> (cells*10 ¹¹ m ⁻²)	non-pigs (cells*10 ¹¹ m ⁻²)	¹⁴ C-PP (mmol C m ⁻² h ⁻¹)	BP: ¹⁴ C-PP (%)
0–45	360 ± 116 (143–622)	576 ± 204 (197–1003)	86 ± 16 (65–111)	214 ± 26 (179–282)	2.0 ± 0.4 (1.2–3.2)	6 ± 2 (2–9)
75–125	181 ± 64 (102–316)	299 ± 134 (90–573)	74 ± 19 (38–110)	207 ± 21 (171–235)	0.7 ± 0.2 (0.3–1.2)	9 ± 4 (4–22)
0–125	739 ± 204 (313–1198)	1198 ± 387 (384–1893)	222 ± 33 (175–276)	562 ± 46 (478–670)	3.6 ± 0.5 (2.7–4.6)	7 ± 2 (3–9)

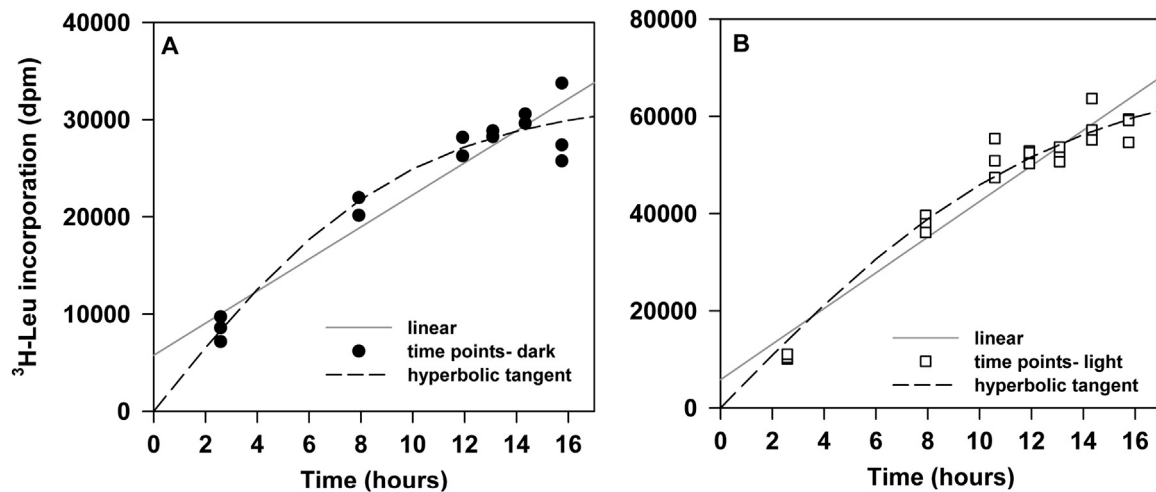


Fig. 2. Representative time-course experiment conducted on HOT 252 (May 2013) depicting disintegrations per minute (dpm) as a function of time measured during the $^3\text{H-Leu}_{\text{Dark}}$ (panel A) and $^3\text{H-Leu}_{\text{Light}}$ (panel B) incubations. Also shown are the least squares regression fits for linear (solid grey line) and hyperbolic tangent models (dashed black line).

test; $p > 0.05$); however, the resulting depth-integrated (0–125 m) rates of $^3\text{H-Leu}_{\text{Light}}$ were significantly lower in 2012 than in 2011 (t -test; $p > 0.001$). Consequently, L:D ratios of the depth-integrated (0–125 m) rates from early 2011 through July 2012 averaged 1.8, while L:D ratios after July 2012 averaged 1.2. Throughout the study period, rates of $^3\text{H-Leu}_{\text{Dark}}$ and $^3\text{H-Leu}_{\text{Light}}$ demonstrated a significant linear relationship (Model II linear regression; $r^2 = 0.45$; $p < 0.0001$; Table 2).

The resulting depth-integrated rates of $^{14}\text{C-PP}$ during this study in the upper euphotic zone (0–45 m) were greater than those in the lower euphotic zone (75–125 m; t -test; $p < 0.0001$; Table 1). Rates of $^{14}\text{C-PP}$ in the upper euphotic zone (< 45 m) ranged 19–84 $\text{nmol C L}^{-1} \text{h}^{-1}$ (averaging $44 \pm 10 \text{ nmol C L}^{-1} \text{h}^{-1}$), while rates in the lower euphotic zone (75–125 m) ranged 1–41 $\text{nmol C L}^{-1} \text{h}^{-1}$ (averaging $14 \pm 9 \text{ nmol C L}^{-1} \text{h}^{-1}$). Rates of $^{14}\text{C-PP}$ did not demonstrate statistically significant interannual differences between 2011 and 2012 (t -test; $p > 0.05$). Rates of $^{14}\text{C-PP}$ remained relatively elevated during the winter of 2011–2012 (Fig. 4); upper euphotic zone (0–45 m) rates of $^{14}\text{C-PP}$ measured in November 2011 were above the 95% upper confidence intervals derived from 24 years of HOT program measurements for the month of November. This pattern was not observed in rates of either

$^3\text{H-Leu}_{\text{Light}}$ or $^3\text{H-Leu}_{\text{Dark}}$ (Fig. 4). During this study, there was no significant correlation between $^{14}\text{C-PP}$ and rates of either $^3\text{H-Leu}_{\text{Light}}$ or $^3\text{H-Leu}_{\text{Dark}}$ at either 25 or 100 m (Supplementary Table 1) or when depth-integrated (0–125 m) rates were examined. However, when a 3-month lag was applied to rates measured at the 25 m depth horizon, a significant relationship was observed between rates of $^3\text{H-Leu}_{\text{Dark}}$ and $^{14}\text{C-PP}$ at near-monthly time scales (Model II linear regression $p < 0.05$; Table 2). There were no other significant relationships between $^{14}\text{C-PP}$ and lagged monthly rates of $^3\text{H-Leu}_{\text{Light}}$ or $^3\text{H-Leu}_{\text{Dark}}$ (when examining lags of up to 6 months). Rates of ΔLeu at 25 m were significantly related to fluctuations in $^{14}\text{C-PP}$, but the relationship was relatively weak (Model II linear regression $r^2 = 0.16$; $p < 0.001$; Table 2).

3.3. Daily and diel scale variability in rates of $^3\text{H-Leu}$ incorporation and $^{14}\text{C-PP}$

During the summer of 2012, rates of $^3\text{H-Leu}$ incorporation and $^{14}\text{C-PP}$ were measured at 25 m at near-daily time scales to assess potential coupling between these processes. During this period, rates of $^3\text{H-}$

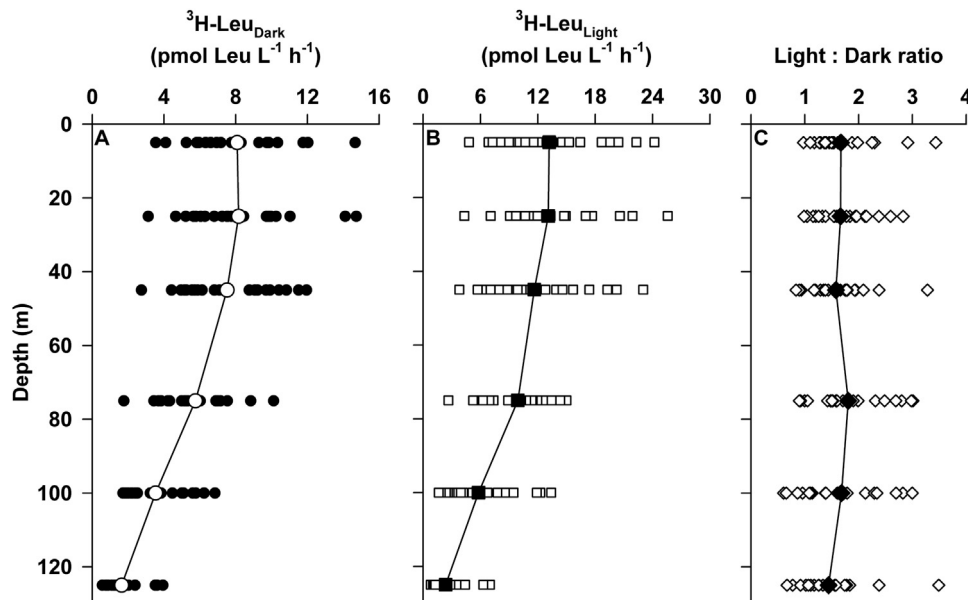


Fig. 3. Depth profiles of $^3\text{H-Leu}_{\text{Dark}}$ (panel A), $^3\text{H-Leu}_{\text{Light}}$ (panel B), and ratio of $^3\text{H-Leu}_{\text{Light}}: ^3\text{H-Leu}_{\text{Dark}}$ (panel C). Individual measurements are given as filled circles ($^3\text{H-Leu}_{\text{Dark}}$), open squares ($^3\text{H-Leu}_{\text{Light}}$), and open diamonds (L:D ratio). Larger symbols connected by lines represent time-averaged mean values.

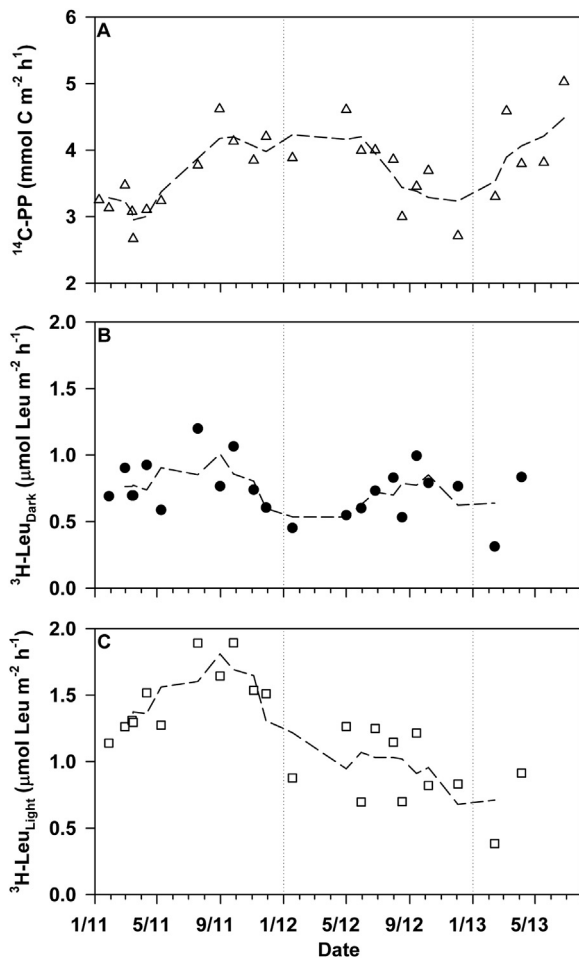


Fig. 4. Depth-integrated (0–125 m) rates of ^{14}C -PP (panel A), ^3H -Leu_{Dark} (panel B), and ^3H -Leu_{Light} (panel C). Dashed lines depict 3-point running mean of each time-series.

Leu_{Dark} and ^3H -Leu_{Light} varied 2- and 2.5-fold, respectively, with ^3H -Leu_{Light} and ^3H -Leu_{Dark} ranging between 6 and 13 pmol Leu $\text{L}^{-1} \text{h}^{-1}$ and 8 and 20 pmol Leu $\text{L}^{-1} \text{h}^{-1}$, respectively (Fig. 5). Over near-daily scales, rates of ^{14}C -PP at 25 m varied 1.8-fold, ranging between 32 and 58 nmol C $\text{L}^{-1} \text{h}^{-1}$ (Fig. 6). Consistent with the near-monthly scale patterns, neither ^3H -Leu_{Dark} nor ^3H -Leu_{Light} were significantly related to daily-scale variations in rates of ^{14}C -PP. We examined linear relationships between rates of ^{14}C -PP and ^3H -Leu_{Light} and ^3H -Leu_{Dark} measured at daily scales over the summer of 2012, including lags of up to seven days, and found no significant relationship between ^{14}C -PP and ^3H -Leu_{Dark} or ^3H -Leu_{Light} at any of those lags (Model II

linear regression, $p > 0.05$). At daily time scales, rates of ΔLeu were weakly, but significantly related to rates of ^{14}C -PP ($r^2 = 0.19$; $p < 0.005$; Table 2). Daily (24-h period) rates of ^3H -Leu incorporation were derived for each cruise from the sum of the ^3H -Leu_{Light} and ^3H -Leu_{Dark} hourly rates multiplied by the respective daylight and night-time periods. The daily rates were then compared to measured rates of ^{14}C -PP by converting to carbon-based estimates of BP assuming 1.5 kg C per mole leucine incorporated (Simon and Azam, 1989). The resulting daily rates of BP ranged 1.0–4.7 mmol C $\text{m}^{-2} \text{d}^{-1}$, equivalent to 3–9% (averaging 7%) of measured rates of ^{14}C -PP (Table 1).

Diel variability in ^3H -Leu incorporation was also examined over a two-day period (August 31 to September 1) during the summer of 2012 (Fig. 7). Rates of ^3H -Leu_{Light} and ^3H -Leu_{Dark} during this diel sampling varied 1.7 and 1.5-fold, respectively, with rates following quasi-sinusoidal patterns. Rates of ^3H -Leu_{Dark} were greatest shortly before sunset or in the early evening, while rates of ^3H -Leu_{Light} were elevated near midday when incident PAR peaked (Fig. 7).

3.4. Statistical relationships between ^3H -Leu incorporation and environmental variability

Statistical analyses revealed no significant correlations in volumetric rates of ^3H -Leu_{Dark} or ^3H -Leu_{Light} and ^{14}C -PP at any of the depths where coincident measurements were conducted ($p > 0.05$; Supplementary Table 1). Similarly, concentrations of chlorophyll *a* and rates of ^3H -Leu_{Dark} or ^3H -Leu_{Light} were not significantly correlated ($p > 0.05$; Supplementary Table 1). In the upper euphotic zone (25 m), variations in temperature at daily to monthly time scales explained 29% and 17% of the variability in rates of ^3H -Leu_{Dark}, and ^3H -Leu_{Light}, respectively ($p < 0.0001$ and $p < 0.001$, respectively; Table 2), while SST explained 24% and 22% of the variability in depth-integrated rates of ^3H -Leu_{Dark}, and ^3H -Leu_{Light} ($p < 0.05$; Table 2). Variations in PAR explained 18% of the variability in upper euphotic zone rates of ^3H -Leu_{Dark} ($r^2 = 0.18$; $p < 0.001$; Table 2), but fluctuations in PAR were not significantly correlated to temporal fluctuations in ^3H -Leu_{Light} ($p > 0.05$). Upper euphotic zone (0–45 m) abundances of *Prochlorococcus* were not correlated with rates of ^3H -Leu_{Light} ($p > 0.05$; Supplementary Table 1), while variability in the combined abundances of *Prochlorococcus* and non-pigmented picoplankton explained 10% of the variability in ^3H -Leu_{Dark} ($p < 0.05$; Table 2). Lower euphotic zone (100 m) and depth-integrated (0–125 m) rates of ^3H -Leu incorporation were not correlated with variations in PAR or temperature ($p > 0.05$; Supplementary Table 1). Abundances of *Prochlorococcus* in the lower (100 m) euphotic zone showed no significant relationships to rates of ^3H -Leu_{Light}, while the variability in combined abundances of *Prochlorococcus* and non-pigmented picoplankton explained 31% of variability in ^3H -Leu_{Dark} ($p < 0.05$; Table 2).

We utilized stepwise linear regression analyses to identify possible

Table 2

Results of Model II linear regression analyses describing relationships among rates of ^3H -Leu_{Light}, ^3H -Leu_{Dark}, ΔLeu , and ^{14}C -PP and variations in temperature (T), PAR, Chlorophyll *a* (Chl *a*), picoplankton abundances (*Prochlorococcus* as [Pro] and non-pigmented picoplankton [non-pigs]), and sea surface temperature (SST). Analyses were conducted for 25 m and 100 m depth horizons and for depth-integrated (0–125 m) rates and stocks. For depth-integrated rates (0–125 m) SST was used for T. Regression analyses not significant at $p < 0.05$ are not shown.

Independent variable	Dependent variable (s)	Depth	Slope	Slope S.D.	Intercept	Intercept S.D.	r^2 -value	p-value	Number of samples
T	^3H -Leu _{Dark}	25 m	2.27	0.29	−48.98	7.23	0.29	< 0.0001	60
T	^3H -Leu _{Light}	25 m	3.93	0.56	−86.36	14.12	0.17	< 0.001	60
PAR	^3H -Leu _{Dark}	25 m	0.90	0.11	−0.23	1.33	0.18	< 0.001	50
^{14}C -PP	^3H -Leu _{Dark} (3 month lag)	25 m	−0.30	0.07	22.88	3.31	0.41	< 0.01	16
^{14}C -PP	ΔLeu	25 m	0.32	0.04	−9.97	2.03	0.16	< 0.001	65
^{14}C -PP (daily, summer 2012)	ΔLeu (daily, summer 2012)	25 m	0.55	0.11	−19.55	5.08	0.19	< 0.005	42
[Pro + non-pigs]	^3H -Leu _{Dark}	25 m	2.27	0.34	7.05	2.39	0.10	< 0.05	61
[Pro + non-pigs]	^3H -Leu _{Dark}	100 m	1.91	0.43	7.61	2.49	0.31	< 0.05	20
^3H -Leu _{Dark}	^3H -Leu _{Light}	0–125 m	1.90	0.35	−205.02	264.53	0.45	< 0.001	22
SST	^3H -Leu _{Dark}	0–125 m	216.97	49.17	−4584.9	1207.5	0.24	< 0.05	22
SST	^3H -Leu _{Light}	0–125 m	411.75	94.63	−8905.6	2323.8	0.22	< 0.05	22

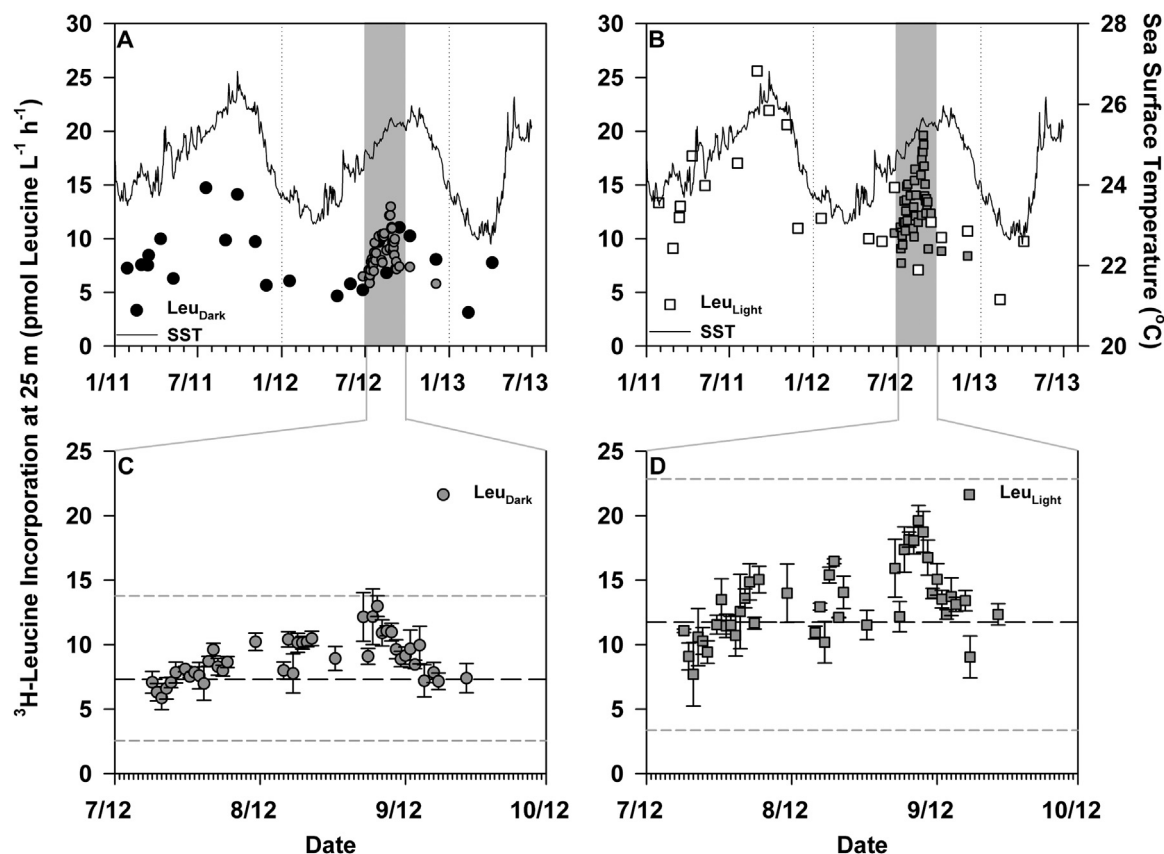


Fig. 5. Time-series of ^3H -Leu_{Dark} (panel A) and ^3H -Leu_{Light} (panel B) measured at 25 m (error bars represent standard deviation of triplicate measurements). Black line represents sea surface temperature (mean daily SST; from WHOI Hawaii Ocean Time-series (WHOTS) mooring (<http://www.soest.hawaii.edu/whots/index.html>)). Lower panels are daily-scale measurements of ^3H -Leu_{Dark} (panel C) and ^3H -Leu_{Light} (panel D) during the summer of 2012. Dashed black line represents time-averaged rates at 25 m depth for the entire period of this study, and dashed grey lines represent upper and lower 95% confidence intervals.

interactions between time-varying changes in measured rates of ^{14}C -PP, ^3H -Leu_{Dark}, and ^3H -Leu_{Light} and temporal fluctuations in PAR, temperature, chlorophyll *a*, and picoplankton abundances. Stepwise multiple linear regression analyses identified interactive relationships between depth-integrated (0–45 m) rates of ^3H -Leu_{Dark} and ^{14}C -PP and mixed layer temperature ($r^2 = 0.72$; $p < 0.001$; Table 3), where temperature alone explained 50% more of the variability in rates of ^3H -Leu_{Dark} than ^{14}C -PP. Results from these analyses also revealed that at the 25 m depth horizon there was a significant interactive relationship between temperature and the combined abundances of *Prochlorococcus* and non-pigmented picoplankton on rates of ^3H -Leu_{Dark} ($r^2 = 0.21$; $p < 0.0001$; Table 3); however, temperature was 80% more powerful than the sum of *Prochlorococcus* and non-pigmented picoplankton in explaining variability in ^3H -Leu_{Dark}.

4. Discussion

Bacterial metabolism plays a central role in ocean carbon cycling (Cho and Azam, 1988; Duarte and Agusti, 1998); however, to date there are relatively few studies examining temporal variability in bacterial growth across multiple scales in the open sea. In the current study, we examined time-variability in rates of ^3H -Leu incorporation over time scales ranging from diel to seasonal in the persistently oligotrophic waters of the NPSG. In addition, by evaluating statistical relationships between ^3H -Leu incorporation and ^{14}C -PP, we sought to better understand temporal coupling between contemporaneous rates of BP and PP in this habitat, and gain insight into factors regulating productivity in this ecosystem.

Previous work has suggested that aquatic bacterial growth can be controlled either by limited supply of organic substrates or by low

temperatures (Shiah and Ducklow, 1994). Our regression analyses identified relatively strong, interactive relationships between temperature and ^{14}C -PP as possible regulators of ^3H -Leu_{Dark} incorporation in the well-lit regions of the euphotic zone (0–45 m), highlighting what may be an important dynamic between resource availability and temperature as co-regulators of BP in this ecosystem. Temperature was positively related to rates of ^3H -Leu_{Dark}. We also considered the combined effect of temperature and ^{14}C -PP together on ^3H -Leu_{Dark}, and when we controlled for the effect of temperature, rates of ^{14}C -PP were inversely related to ^3H -Leu_{Dark}. These results, when coupled with the observation that in the near-surface waters rates of ^3H -Leu_{Dark} appear to lag rates of ^{14}C -PP (by up to 3 months), suggest that during late summer and fall when bacterial abundance is greatest and rates of ^{14}C -PP have begun to decline, increasing temperatures stimulate BP. Similar relationships between ^3H -Leu incorporation and temperature were not observed below the mixed layer, where temperatures are considerably more time variable. Lower euphotic zone temperature variability does not exhibit significant seasonality, undergoing higher frequency forcing by meso- and submesoscale physical forcing (Church et al., 2009). In well-lit regions of the euphotic zone, temporal fluctuations in PAR also appeared significantly related to rates of ^3H -Leu_{Dark}, although changes in PAR explained less of the variability in ^3H -Leu_{Dark} than temperature.

We derived daily rates of BP as the sum of the ^3H -Leu_{Light} and ^3H -Leu_{Dark} hourly rates multiplied by the respective daylight and nighttime periods for each cruise. This assumes the ^3H -Leu_{Dark} rates approximate nighttime rates of BP. Our diel scale sampling of ^3H -Leu (Fig. 7) suggests rates of ^3H -Leu_{Dark} increase ~25% in the early evening, so the daily rates of BP derived by this approach are likely to be underestimates. The resulting carbon-based rates of daily BP

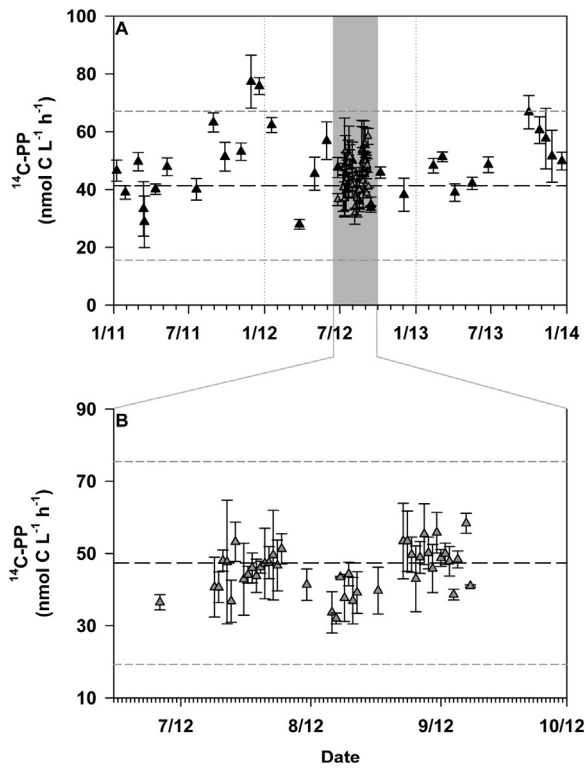


Fig. 6. Time-series of ^{14}C -PP measured at 25 m during this study (panel A); dashed black line depicts the mean time-averaged rate of ^{14}C -PP measured by the HOT program for this depth; dashed grey lines represent 95% confidence intervals for these measurements. Also shown are rates of ^{14}C -PP at 25 m measured during summer 2012 (panel B). The mean HOT program derived rate of ^{14}C -PP (1988–2014) for July, August, and September is shown as a black dashed line, with the associated 95% confidence intervals shown as grey dashed lines.

averaged $2.9 \pm 0.8 \text{ mmol C m}^{-2} \text{ d}^{-1}$, equivalent to 3–9% of contemporaneous ^{14}C -PP. This ratio is similar to the BP:PP ratios of 5% reported by Ducklow et al. (2012) and ratios reported at BATS (Steinberg et al., 2001; Carlson et al., 1996), but are somewhat low compared to the 10–30% reported in other regions of the open sea (Anderson and Ducklow, 2001; Cole et al., 1988; del Giorgio et al., 1997; Ducklow, 1999; Hoppe et al., 2002).

A recent study reported rates of euphotic zone microbial community respiration (R) measured in the dark at Station ALOHA between 2011 and 2012 (a period overlapping our study) that averaged $41.2 \pm 8.7 \text{ mmol C m}^{-2} \text{ d}^{-1}$ (based on 0–125 m depth-integrated rates estimated for 0.2–0.8 μm size fractionated plankton (Martínez-García and Karl, 2015)). Assuming the $<0.8 \mu\text{m}$ measurements of R from this study reflect activities of bacterioplankton, combining these data with our measurements of BP suggests bacterial carbon demand ($\text{BCD} = \text{BP} + \text{R}$) during this period was upwards of $44 \pm 9 \text{ mmol C m}^{-2} \text{ d}^{-1}$, equivalent to $100\% \pm 27\%$ of the contemporaneous measurements of ^{14}C -PP. These analyses also imply a bacterial growth efficiency ($\text{BGE} = \text{BP} / \text{BCD}$) of $7 \pm 2\%$. BGEs for marine bacteria have been reported to range between 5–40% (Carlson et al., 1999; Carlson and Ducklow, 1996; del Giorgio et al., 1997; del Giorgio and Cole, 1998), with BGE often lower in oligotrophic relative to more eutrophic marine ecosystems (Carlson and Ducklow, 1996; del Giorgio and Cole, 1998). Hence, although our measurements revealed that a relatively low fraction of contemporaneous ^{14}C -PP supports BP at Station ALOHA, based on these estimates of BGE, the daily flux of carbon supporting bacterial metabolism appears to be a major pathway for primary production in this ecosystem. Moreover, statistical analyses of the relationships between ^3H -Leu and ^{14}C -PP revealed an apparent temporal lag between BP and PP, with BP regulated through the interactive influences of PP and temperature. Such results may imply temporal

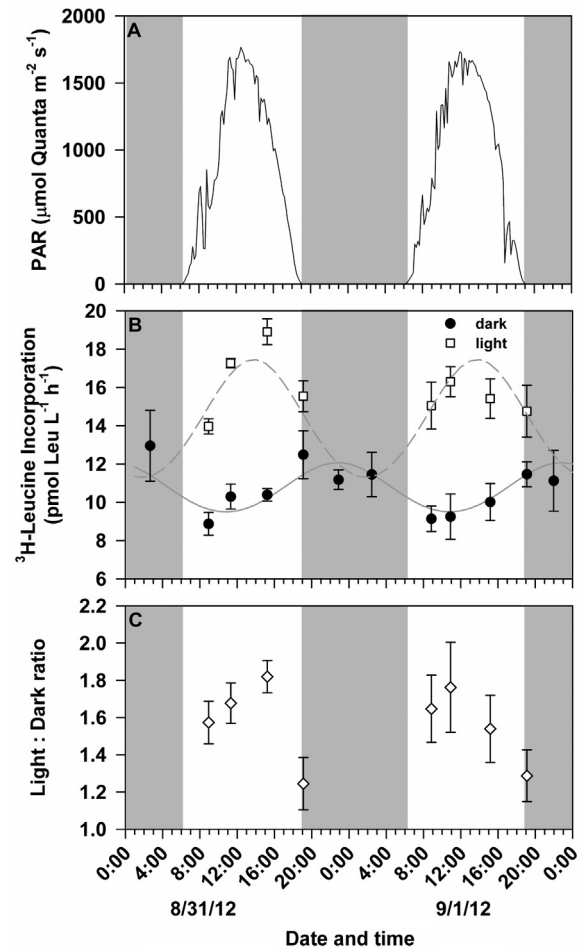


Fig. 7. Diel variability in rates of ^3H -Leu incorporation (both light and dark) measured at 25 m during the summer of 2012. Grey bars represent night periods. Daily variation in incident PAR (panel A), ^3H -Leu_{Light} and ^3H -Leu_{Dark} (panel B), and L:D ratio (panel C). Error bars represent standard deviations of triplicate measurements at each time point. Grey line depicts sinusoidal model fit ($r^2 = 0.64$) from John et al. (2011).

Table 3

Results of stepwise multiple linear regression analyses evaluating relationships among rates of ^3H -Leu_{Light}, ^3H -Leu_{Dark}, and ^{14}C -PP and variations in temperature (T), PAR, Chlorophyll *a* (Chl *a*), and picoplankton abundances (*Prochlorococcus* as [Pro] and non-pigmented picoplankton as [non-pigs]). Analyses were conducted for 25 m and 100 m depth horizons and for depth-integrated rates (0–45 m and 0–125 m), where sea surface temperature (SST) was used for T. Regression analyses not significant at $p < 0.05$ are not shown. Standardized partial regression coefficients are given for both significant independent variables, separated by commas. Best fit factor coefficient is listed first.

Dependent variable	Depth	Significant independent variables	Best fit factor	Standardized partial regression coefficients	r^2
^3H -Leu _{Dark}	25	T, [Pro + non-pigs]	T	0.52, 0.29	0.31
^3H -Leu _{Dark}	0–45 m	T, ^{14}C -PP	T	0.85, -0.55	0.72
^{14}C -PP	0–125 m	PAR, Chl <i>a</i>	PAR	0.74, 0.61	0.55

shifts in the partitioning of photosynthetic organic matter production between dissolved and particulate pools. In particular, during the early fall when upper ocean temperatures are maximal, phytoplankton may partition a larger fraction of daily production into DOM relative to production of cellular material. However, time-series measurements of DOC production at Station ALOHA suggest no seasonal dependence in the partitioning of primary production between particulate and dissolved phases (Viviani et al., 2015). Temporal decoupling between maximal PP and BP over several weeks to months has also been

observed at BATS (Steinberg et al., 2001), suggesting that this pattern may be a common feature of oligotrophic ecosystems. This decoupling may derive from seasonal-scale shifts in the nutritional and energetic content of photosynthetically produced DOM. Alternatively, the temporally lagged response in BP relative to PP observed in the present study may suggest bacterial growth during the fall depends on excess phytoplankton production that occurs during the summer months, highlighting a potential role for semi-labile DOM in supporting bacterial growth in the upper ocean of this ecosystem.

By conducting parallel ^3H -Leu incubations in both the dark and light, we examined how vertical and time-varying changes in irradiance influenced rates of bacterial protein production. Consistent with previous reports (Church et al., 2006, 2004), we found that upper ocean (< 125 m) rates of ^3H -Leu_{Light} were consistently greater than ^3H -Leu_{Dark} by 1.5-fold, on average, a finding consistent with incorporation of ^3H -Leu by *Prochlorococcus* (Michelou et al., 2007; Zubkov et al., 2004; Zubkov and Tarran, 2005). Despite large changes in the vertical flux of light through the upper ocean, we observed no consistent depth-dependent patterns to the photostimulation of ^3H -Leu incorporation. In a recent study, Björkman et al. (2015) quantified rates of ^3H -Leu incorporation by both *Prochlorococcus* and non-pigmented picoplankton at Station ALOHA based on flow cytometric sorting of radiolabeled cells. These authors report that ~60% of the ^3H -Leu incorporation that occurred in the light was attributable to assimilation by *Prochlorococcus*, with rates of ^3H -Leu incorporation by these cyanobacteria 7-fold greater (on average) in the light than in the dark. In contrast, *Prochlorococcus* contributed ~20% of the total ^3H -Leu incorporation in the dark (Björkman et al., 2015), slightly less than the average proportional contribution of these cells to total picoplankton abundances (*Prochlorococcus* averages 26% of the total picoplankton cell inventories at Station ALOHA).

The extent to which *Prochlorococcus* relies on organic matter to supplement autotrophic production remains unclear; however, *Prochlorococcus* is responsible for a large fraction of daily net primary productivity in the NPSG (Liu et al., 1997) and demonstrates relatively high per cell rates of ^3H -Leu incorporation (Björkman et al., 2015). In the current study, rates of ^3H -Leu_{Light} were lower in 2012 relative to the previous year, while rates of ^3H -Leu_{Dark} were generally similar. The resulting ^3H -Leu L:D ratio decreased by ~25% between these years; these changes coincided with a period where *Prochlorococcus* cell abundances and rates of primary productivity were anomalously low for this region (Wilson et al., 2015). Together these findings suggest variability in the biomass and growth of *Prochlorococcus* exerts substantial control over upper ocean carbon cycling in this ecosystem. The lack of relationship between *Prochlorococcus* cell abundance and ΔLeu suggests variability in the rates of ^3H -Leu_{Light} reflects variations in *Prochlorococcus* growth rather than fluctuations in biomass. In contrast, the observed relationship between ^3H -Leu_{Dark} and the summed abundances of non-pigmented picoplankton and *Prochlorococcus*, suggests that time-varying changes in the population sizes of these organisms regulates rates of ^3H -Leu_{Dark}. Thus BP in this oligotrophic ecosystem appears driven by a combination of temporally variable rates of light enhanced growth by *Prochlorococcus*, superimposed over a less variable heterotrophic metabolism that appears partly controlled by variations in temperature, cellular abundance, and resource availability.

During the summer of 2012 we examined diel- to daily-scale fluctuations in rates of ^3H -Leu incorporation. Over diel-scales, rates of ^3H -Leu_{Dark} and ^3H -Leu_{Light} oscillated by 1.5- and 1.7-fold, respectively, while day-to-day changes in these rates varied approximately 2- and 2.5-fold, respectively. Diel-scale measurements indicated rates of ^3H -Leu_{Dark} were greatest at or near dusk, consistent with observations from the tropical Atlantic (Mary et al., 2008). In other studies, for example the North Sea (Winter et al., 2004) and Southern California Bight (Fuhrman et al., 1985) BP was higher during day than at night, while studies in more eutrophic freshwater and coastal systems

identified no consistent diel pattern in BP (Riemann and Søndergaard, 1984). In contrast, our observations that rates of ^3H -Leu_{Light} peak near noon supports the notion that photostimulation of ^3H -Leu incorporation is likely controlled by variations in *Prochlorococcus* growth. Our results also appear consistent with studies suggesting that phytoplankton and heterotrophic bacteria may exhibit synchronous activity, with *Prochlorococcus* transcriptional maxima of photosystem genes followed on the order of hours by a succession of transcript maxima in oxidative phosphorylation genes among heterotrophic bacteria (Aylward et al., 2015; Ottesen et al., 2014).

4.1. Conclusions

In summary, we observed consistent, albeit temporally decoupled, daily patterns of ^3H -Leu incorporation in the light and the dark. Such results likely reflect the coupling between photosynthetic production of organic matter and subsequent bacterial growth over diel to daily time scales. In contrast, over weekly to monthly scales, variability in measured rates of ^{14}C -PP was relatively constant (varying < 2-fold) across daily to monthly scales, while rates of ^3H -Leu incorporation generally demonstrated greater variability at these time scales (5- and 4-fold variability in light and dark, respectively). Moreover, statistical evaluation of the measured rates of ^3H -Leu incorporation and ^{14}C -PP together with coincident measurements of environmental variability (including temperature, light, picoplankton abundances, and chlorophyll) revealed that temporal fluctuations in ^{14}C -PP, temperature, and bacterial abundance (inclusive of both non-pigmented picoplankton and *Prochlorococcus*) were significant controls on bacterial growth in the well-lit regions of the euphotic zone. Such results highlight the complexity of interacting processes that appear to regulate BP and PP in this ecosystem, and reinforce the value of examining coupling in these processes across multiple, nested time scales.

Author contributions

Both DAV and MJC contributed to the design of the project; DAV conducted the sampling and laboratory analyses, and both authors contributed to the analyses of data and writing of the manuscript.

Acknowledgements

Funding for this study derived from the National Science Foundation (NSF), including grants OCE-0850827 and OCE-1260164 to MJC. Additional support was provided by NSF through the Center for Microbial Oceanography: Research and Education (CMORE; EF-0424599) and the Simons Collaboration on Ocean Processes and Ecology (SCOPE award ID 329108). We thank the scientists and staff of the HOT program for their assistance at sea and in the laboratory, and Dr. Sam Wilson (UH) for his leadership during the HOE DYLAN cruises. Drs. Craig Nelson (UH) and David Karl (UH) provided comments that improved this manuscript. An anonymous reviewer provided thoughtful comments that further improved this work. We extend our gratitude to the officers and crew of the R/V *Kilo Moana* and the R/V *Kaimikai-o-Kanaloa*.

Appendix A. Supplementary information

Supplementary information associated with this article can be found in the online version at doi:10.1016/j.dsr.2017.01.006.

References

- Alonso-Sáez, L., Vázquez-Domínguez, E., Cardelús, C., Pinhassi, J., Sala, M.M., Lekunberri, I., Balagué, V., Vila-Costa, M., Unrein, F., Massana, R., Simó, R., Gasol, J.M., 2008. Factors controlling the year-round variability in carbon flux through

- bacteria in a coastal marine system. *Ecosystems* 11, 397–409. <http://dx.doi.org/10.1007/s10021-008-9129-0>.
- Anderson, T., Ducklow, H., 2001. Microbial loop carbon cycling in ocean environments studied using a simple steady-state model. *Aquat. Microb. Ecol.* 26, 37–49. <http://dx.doi.org/10.3354/ame026037>.
- Aylward, F.O., Eppley, J.M., Smith, J.M., Chavez, F.P., Scholin, C.A., DeLong, E.F., 2015. Microbial community transcriptional networks are conserved in three domains at ocean basin scales. *Proc. Natl. Acad. Sci. USA* 112, 5443–5448. <http://dx.doi.org/10.1073/pnas.1502883112>.
- Azam, F., Fenchel, T., Field, J., Gray, J., Meyer-Reil, L., Thingstad, F., 1983. The ecological role of water-column microbes in the sea. *Mar. Ecol. Prog. Ser.* 10, 257–263.
- Behrenfeld, M.J., Falkowski, P.G., 1997. Photosynthetic rates derived from satellite-based chlorophyll concentration. *Limnol. Oceanogr.* 42, 1–20.
- Billen, G., Servais, P., Becquevort, S., 1990. Dynamics of bacterioplankton in oligotrophic and eutrophic aquatic environments: bottom-up or top-down control? *Hydrobiologia* 207, 37–42. <http://dx.doi.org/10.1007/BF00041438>.
- Björkman, K.M., Church, M.J., Doggett, J.K., Karl, D.M., 2015. Differential assimilation of inorganic carbon and leucine by *Prochlorococcus* in the oligotrophic North Pacific Subtropical Gyre. *Front. Microbiol.* 6, 1401. <http://dx.doi.org/10.3389/fmicb.2015.01401>.
- Burnham, K.P., Anderson, D.R., Huyvaert, K.P., 2010. AIC model selection and multimodel inference in behavioral ecology: some background, observations, and comparisons. *Behav. Ecol. Sociobiol.* 65, 23–35. <http://dx.doi.org/10.1007/s00265-010-1029-6>.
- Campbell, L., Nolla, H.A., Vault, D., 1994. The importance of *Prochlorococcus* to community structure in the central North Pacific Ocean. *Limnol. Oceanogr.* 39, 954–961.
- Carlson, C., Ducklow, H., Michaels, A., 1994. Annual flux of dissolved organic carbon from the euphotic zone in the northwestern Sargasso Sea. *Nature* 371, 405–408.
- Carlson, C.A., Ducklow, H.W., 1996. Growth of bacterioplankton and consumption of dissolved organic carbon in the Sargasso Sea. *Aquat. Microb. Ecol.* 10, 69–85. <http://dx.doi.org/10.3354/ame010069>.
- Carlson, C.A., Ducklow, H.W., Sleeter, T.D., 1996. Stocks and dynamics of bacterioplankton in the northwestern Sargasso Sea. *Deep Sea Res. II* 43, 491–515. [http://dx.doi.org/10.1016/0967-0645\(95\)00101-8](http://dx.doi.org/10.1016/0967-0645(95)00101-8).
- Carlson, C.A., Bates, N.R., Ducklow, H.W., Hansell, D.A., 1999. Estimation of bacterial respiration and growth efficiency in the Ross Sea, Antarctica. *Aquat. Microb. Ecol.* 19, 229–244.
- Cho, B.C., Azam, F., 1988. Major role of bacteria in biogeochemical fluxes in the ocean's interior. *Nature* 332, 441–443. <http://dx.doi.org/10.1038/332441a0>.
- Church, M., Ducklow, H., Karl, D., 2004. Light dependence of [^3H]leucine incorporation in the oligotrophic North Pacific ocean. *Appl. Environ. Microbiol.* 70, 4079–4087.
- Church, M., Ducklow, H., Letelier, R., Karl, D., 2006. Temporal and vertical dynamics in picoplankton phototrophic production in the subtropical North Pacific Ocean. *Aquat. Microb. Ecol.* 45, 41–53.
- Church, M.J., 2008. Resource control of bacterial dynamics in the sea. In: Kirchman, D.L. (Ed.), *Microbial Ecology of the Oceans*. John Wiley & Sons, Inc, Hoboken, NJ, USA, 335–382.
- Church, M.J., Mahaffey, C., Letelier, R.M., Lukas, R., Zehr, J.P., Karl, D.M., 2009. Physical forcing of nitrogen fixation and diazotroph community structure in the North Pacific subtropical gyre. *Glob. Biogeochem. Cycles* 23, GB2020. <http://dx.doi.org/10.1029/2008GB003418>.
- Church, M.J., Lomas, M.W., Muller-Karger, F., 2013. Sea change: charting the course for biogeochemical ocean time-series research in a new millennium. *Deep Sea Res. II* 93, 2–15. <http://dx.doi.org/10.1016/j.dsr2.2013.01.035>.
- Cole, J., Findlay, S., Pace, M., 1988. Bacterial production in fresh and saltwater ecosystems - a cross-system overview. *Mar. Ecol. Prog. Ser.* 43, 1–10. <http://dx.doi.org/10.3354/meps043001>.
- Cotner, J.B., Biddanda, B.A., 2002. Small players, large role: microbial influence on biogeochemical processes in pelagic aquatic ecosystems. *Ecosystems* 5, 105–121. <http://dx.doi.org/10.1007/s10021-001-0059-3>.
- Duarte, C., Cebrían, J., 1996. The fate of marine autotrophic production. *Limnol. Oceanogr.* 41, 1758–1766.
- Duarte, C., Agustí, S., 1998. The CO_2 balance of unproductive aquatic ecosystems. *Science* 281, 234–236.
- Ducklow, H., 1999. The bacterial component of the oceanic euphotic zone. *FEMS Microbiol. Ecol.* 30, 1–10.
- Ducklow, H.W., Schofield, O.M.E., Vernet, M., Stammerjohn, S.E., Erickson, M., 2012. Multiscale control of bacterial production by phytoplankton dynamics and sea ice along the western Antarctic Peninsula: a regional and decadal investigation. *J. Mar. Syst.* 98, 26–39.
- Ducklow, H., Carlson, C., 1992. Oceanic bacterial production. In: *Advances in Microbial Ecology*. Springer, USA, pp. 113–181.
- Field, C.B., Behrenfeld, M.J., Randerson, J.T., Falkowski, P., 1998. Primary production of the biosphere: integrating terrestrial and oceanic components. *Science* 281, 237–240. <http://dx.doi.org/10.1126/science.281.5374.237>.
- Fouilland, E., Tolosa, I., Bonnet, D., Bouvier, C., Bouvier, T., Bouvy, M., Got, P., Floch, E.L., Mostajir, B., Roques, C., Sempéré, R., Sime-Ngando, T., Vidussi, F., 2014. Bacterial carbon dependence on freshly produced phytoplankton exudates under different nutrient availability and grazing pressure conditions in coastal marine waters. *FEMS Microbiol. Ecol.* 87, 757–769. <http://dx.doi.org/10.1111/1574-6941.12262>.
- Fuhrman, J.A., Eppley, R.W., Hagström, Å., Azam, F., 1985. Diel variations in bacterioplankton, phytoplankton, and related parameters in the Southern California Bight. *Mar. Ecol. Prog. Ser.* 27, 9–20.
- del Giorgio, P., Cole, J., 1998. Bacterial growth efficiency in natural aquatic systems. *Ann. Rev. Mar. Sci.* 29, 503–541.
- del Giorgio, P., Cole, J., Cimbleris, A., 1997. Respiration rates in bacteria exceed phytoplankton production in unproductive aquatic systems. *Nature* 385, 148–151.
- Hansell, D., Carlson, C., 1998. Net community production of dissolved organic carbon. *Glob. Biogeochem. Cycles* 12, 443–453.
- Hoppe, H.-G., Gocke, K., Koppe, R., Begler, C., 2002. Bacterial growth and primary production along a north–south transect of the Atlantic Ocean. *Nature* 416, 168–171. <http://dx.doi.org/10.1038/416168a>.
- John, D.E., López-Díaz, J.M., Cabrera, A., Santiago, N.A., Corredor, J.E., Bronk, D.A., Paul, J.H., 2011. A day in the life in the dynamic marine environment: how nutrients shape diel patterns of phytoplankton photosynthesis and carbon fixation gene expression in the Mississippi and Orinoco River plumes. *Hydrobiologia* 679, 155–173. <http://dx.doi.org/10.1007/s10750-011-0862-6>.
- Joint, I., Pomroy, A., 1987. Activity of heterotrophic bacteria in the euphotic zone of the Celtic Sea. *Mar. Ecol. Prog. Ser.* 41, 155–165.
- Karl, D., 1999. A sea of change: biogeochemical variability in the North Pacific Subtropical Gyre. *Ecosystems* 2, 181–214.
- Karl, D., Lukas, R., 1996. The Hawaii Ocean Time-series (HOT) program: background, rationale and field implementation. *Deep Sea Res. II* 43, 129–156.
- Karl, D., Hebel, D., Björkman, K., Letelier, R., 1998. The role of dissolved organic matter release in the productivity of the oligotrophic North Pacific Ocean. *Limnol. Oceanogr.* 43, 1270–1286.
- Karl, D.M., Björkman, K.M., Dore, J.E., Fujieki, L., Hebel, D.V., Houlihan, T., Letelier, R.M., Tupas, L.M., 2001. Ecological nitrogen-to-phosphorus stoichiometry at station ALOHA. *Deep Sea Res. II* 48, 1529–1566. [http://dx.doi.org/10.1016/S0967-0645\(00\)00152-1](http://dx.doi.org/10.1016/S0967-0645(00)00152-1).
- Karl, D.M., Church, M.J., Dore, J.E., Letelier, R.M., Mahaffey, C., 2012. Predictable and efficient carbon sequestration in the North Pacific Ocean supported by symbiotic nitrogen fixation. *Proc. Natl. Acad. Sci. USA* 109, 1842–1849. <http://dx.doi.org/10.1073/pnas.1120312109>.
- Kirchman, D., K'nees, E., Hodson, R., 1985. Leucine incorporation and its potential as a measure of protein synthesis by bacteria in natural aquatic systems. *Appl. Environ. Microbiol.* 49, 599–607.
- Kirchman, D., Newell, S., Hodson, R., 1986. Incorporation versus biosynthesis of leucine - implications for measuring rates of protein-synthesis and biomass production by bacteria. *Mar. Ecol. Prog. Ser.* 32, 47–59. <http://dx.doi.org/10.3354/meps032047>.
- Kirchman, D.L., 2004. A primer on dissolved organic material and heterotrophic prokaryotes in the oceans. In: Follows, M., Oguz, T. (Eds.), *The Ocean Carbon Cycle and Climate* (NATO Science Series). Springer, Netherlands, 31–63.
- Letelier, R., Dore, J., Winn, C., Karl, D., 1996. Seasonal and interannual variations in photosynthetic carbon assimilation at Station ALOHA. *Deep Sea Res. II* 43, 467–490.
- Letelier, R., Karl, D., Abbott, M., Bidigare, R., 2004. Light driven seasonal patterns of chlorophyll and nitrate in the lower euphotic zone of the North Pacific Subtropical Gyre. *Limnol. Oceanogr.* 49, 508–519.
- Liu, H., Nolla, H., Campbell, L., 1997. *Prochlorococcus* growth rate and contribution to primary production in the equatorial and subtropical North Pacific Ocean. *Aquat. Microb. Ecol.* 12, 39–47. <http://dx.doi.org/10.3354/ame012039>.
- Marra, J., 2009. Net and gross productivity: weighing in with ^{14}C . *Aquat. Microb. Ecol.* 56, 123–131.
- Martínez-García, S., Karl, D.M., 2015. Microbial respiration in the euphotic zone at Station ALOHA. *Limnol. Oceanogr.* 60, 1039–1050. <http://dx.doi.org/10.1002/lno.10072>.
- Mary, I., Garcezarek, L., Tarran, G.A., Kolowrat, C., Terry, M.J., Scanlan, D.J., Burkil, P.H., Zubkov, M.V., 2008. Diel rhythmicity in amino acid uptake by *Prochlorococcus*. *Environ. Microbiol.* 10, 2124–2131. <http://dx.doi.org/10.1111/j.1462-2920.2008.01633.x>.
- Michaels, A., Bates, N., Buesseler, K., Carlson, C., Knap, A., 1994. Carbon-cycle imbalances in the Sargasso Sea. *Nature* 372, 537–540.
- Michelou, V.K., Cottrell, M.T., Kirchman, D.L., 2007. Light-stimulated bacterial production and amino acid assimilation by cyanobacteria and other microbes in the North Atlantic Ocean. *Appl. Environ. Microbiol.* 73, 5539–5546. <http://dx.doi.org/10.1128/AEM.00212-07>.
- Ottesen, E.A., Young, C.R., Gifford, S.M., Eppley, J.M., Marin, R., Schuster, S.C., Scholin, C.A., DeLong, E.F., 2014. Multispecies diel transcriptional oscillations in open ocean heterotrophic bacterial assemblages. *Science* 345, 207–212. <http://dx.doi.org/10.1126/science.1252476>.
- Pace, M.L., Cole, J.J., 1994. Primary and bacterial production in lakes: are they coupled over depth? *J. Plankton Res.* 16, 661–672. <http://dx.doi.org/10.1093/plankt/16.6.661>.
- Pace, M.L., del Giorgio, P., Fischer, D., Condon, R., Malcom, H., 2004. Estimates of bacterial production using the leucine incorporation method are influenced by differences in protein retention of microcentrifuge tubes. *Limnol. Oceanogr.* Methods 2, 55–61. <http://dx.doi.org/10.4319/lom.2004.2.55>.
- Pomeroy, L.R., 1974. The ocean's food web, a changing paradigm. *BioScience* 24, 499–504. <http://dx.doi.org/10.2307/1296885>.
- R Development Core Team, 2008. R: A Language and Environment for Statistical Computing. R Foundation for Statistical Computing, Vienna, Austria.
- Riemann, B., Sondergaard, M., 1984. Measurements of diel rates of bacterial secondary production in aquatic environments. *Appl. Environ. Microbiol.* 47, 632–638.
- Rii, Y.M., Karl, D.M., Church, M.J., 2016. Temporal and vertical variability in picophytoplankton primary productivity in the North Pacific Subtropical Gyre. *Mar. Ecol. Prog. Ser.* 562, 1–18.
- Shiah, F., Ducklow, H., 1994. Temperature regulation of heterotrophic bacterioplankton abundance, production, and specific growth-rate in Chesapeake Bay. *Limnol. Oceanogr.* 39, 1243–1258.

- Simon, M., Azam, F., 1989. Protein content and protein synthesis rates of planktonic marine bacteria. *Mar. Ecol. Prog. Ser.* 51, 201–213. <http://dx.doi.org/10.3354/meps051201>.
- Smith, D.C., Azam, F., 1992. A simple, economical method for measuring bacterial protein synthesis rates in seawater using ^3H -leucine. *Mar. Microb. Food Webs* 6, 107–114.
- Steemann Nielsen, E., 1952. The use of radio-active carbon (C^{14}) for measuring organic production in the sea. *J. Cons. Int. Explor. Mer.* 18, 117–140. <http://dx.doi.org/10.1093/icesjms/18.2.117>.
- Steinberg, D.K., Carlson, C.A., Bates, N.R., Johnson, R.J., Michaels, A.F., Knap, A.H., 2001. Overview of the US JGOFS Bermuda Atlantic Time-series Study (BATS): a decade-scale look at ocean biology and biogeochemistry. *Deep Sea Res II* 48, 1405–1447, (doi:16/S0967-0645(00)(00148-X).
- Van Wambeke, F.V., Obernosterer, I., Moutin, T., Duhamel, S., Ulloa, O., Claustre, H., 2008. Heterotrophic bacterial production in the eastern South Pacific: longitudinal trends and coupling with primary production. *Biogeosciences* 5, 157–169.
- Viviani, D.A., Karl, D.M., Church, M.J., 2015. Variability in photosynthetic production of dissolved and particulate organic carbon in the North Pacific Subtropical Gyre. *Front. Mar. Sci.* 2, 73. <http://dx.doi.org/10.3389/fmars.2015.00073>.
- Wilson, S.T., Barone, B., Ascani, F., Bidigare, R.R., Church, M.J., del Valle, D.A., Dyhrman, S.T., Ferrón, S., Fitzsimmons, J.N., Juranek, L.W., Kolber, Z.S., Letelier, R.M., Martínez-García, S., Nicholson, D.P., Richards, K.J., Rii, Y.M., Rouco, M., Viviani, D.A., White, A.E., Zehr, J.P., Karl, D.M., 2015. Short-term variability in euphotic zone biogeochemistry and primary productivity at Station ALOHA: a case study of summer 2012. *Glob. Biogeochem. Cycles* 29. <http://dx.doi.org/10.1002/2015GB005141>.
- Winter, C., Herndl, G.J., Weinbauer, M.G., 2004. Diel cycles in viral infection of bacterioplankton in the North Sea. *Aquat. Microb. Ecol.* 35, 207–216.
- Zar, J.H., 1999. *Biostatistical Analysis*. Prentice Hall PTR, New Jersey.
- Zubkov, M.V., Tarran, G.A., 2005. Amino acid uptake of *Prochlorococcus* spp. in surface waters across the South Atlantic Subtropical Front. *Aquat. Microb. Ecol.* 40, 241–249.
- Zubkov, M.V., Tarran, G.A., Fuchs, B.M., 2004. Depth related amino acid uptake by *Prochlorococcus* cyanobacteria in the Southern Atlantic tropical gyre. *FEMS Microbiol. Ecol.* 50, 153–161. <http://dx.doi.org/10.1016/j.femsec.2004.06.009>.